

# Radially polarized, actively Q-switched, and end-pumped Nd:YAG laser

K.G. Xia · K.-I. Ueda · J.L. Li

Received: 24 August 2011 / Revised version: 24 October 2011 / Published online: 7 February 2012  
© Springer-Verlag 2012

**Abstract** In this paper, we demonstrated an actively Q-switched, radially polarized, and laser-diode end-pumped Nd:YAG laser with an acousto-optic modulator as the Q switch and a photonic crystal grating as the output coupler. The laser generated pulses of 26.4–67.2 ns duration, and the repetition rate can be continuously adjusted from 500 Hz to 9.238 kHz with peak power up to 7.75 kW. Such a radially polarized pulse would facilitate numerous applications.

## 1 Introduction

Radially polarized beams with a donut shape are characterized by axial symmetry in both amplitude and polarization along the beam axis. Such beams are interesting for several applications, such as orientation of single molecules, optical tweezers [1], particles manipulation [2–4], optical data storage, and resolution-enhanced microscopy [5]. They are also suggested to use in metal processing, including metal cutting, welding, and drilling [6–10]. In material-processing application, the electric field vector of the radial-polarization irradiation is spatially perpendicular to the cutting front irrespective of the direction of cutting, which results in the high Fresnel absorption of metal material and thus ensures a very high overall efficiency.

The benefits mentioned above have drawn increasing attention to radially polarized laser sources. In recent three decades, many methods have been developed in order to generate such radially polarized lights either inside the laser resonator by using various intracavity polarization-selective elements like subwavelength gratings [11–16], conical prisms [17, 18], and birefringent elements [19] to force the desired oscillation, or outside the laser resonator via interferometer [20] and mode conversion in a few-mode fiber [21] and so on. It is worth mentioning that methods based on subwavelength gratings have greater potential to acquire high-power radially polarization beams with high mode quality and purity. To the best of our knowledge, the largest radial polarization output for both gas lasers and solid-state lasers are based on subwavelength gratings [22, 23].

For practical applications like precise metal processing, highly intensive laser irradiation is necessary to reach or exceed the ablation threshold, and this bring attention to the laser that produces radially polarized laser pulses with high peak power and short duration via Q-switching or mode-locking techniques. For example, Li et al. [15, 24] demonstrated a laser-diode (LD) end-pumped, radially polarized Nd:YAG ceramic microchip laser passively Q-switched by a saturation absorber with a photonics crystal grating as the polarization-selective output coupler. Such a laser was simple and compact, and also the end-pumped configuration provided high mode quality and high laser efficiency; nevertheless this scheme had difficulties in active and accurate control to the pulse frequency and the width unless the active Q switching is used. Furthermore, Feurer et al. [25, 26] reported the lamp-pumped and radially polarized Nd:YAG laser actively Q-switched or mode-locked by an acoustic-optic modulator (AOM) where the thermally-induced birefringence inside the lasing crystal is responsible for the

---

K.G. Xia · J.L. Li (✉)  
Shanghai Institute of Optics and Fine Mechanics, Chinese  
Academy of Sciences, Shanghai 201800, China  
e-mail: [apuli@siom.ac.cn](mailto:apuli@siom.ac.cn)  
Fax: +86-21-69918165

K.-I. Ueda  
Institute for Laser Science, University  
of Electro-communications, Tokyo 182-8585, Japan

polarization-selective mechanism. In the latter case, though the picosecond-duration and high-peak-power pulse could be generated, both the stability region of laser cavity and the favored birefringence were pump-dependent, and thus radially polarized pulse only could be emitted in a limited range of pump powers with specific repetition rate.

In this letter we present a laser-diode (LD) end-pumped, AOM Q-switched, and radially polarized Nd:YAG laser with a photonic crystal grating as the output coupler. The laser's gain medium is bonded with two undoped YAG end caps to weaken the temperature gradient in the lasing area and thereafter the considerable thermal lens effect at the presence of intensive pumping. Moreover, the end-pumping scheme is beneficial to improve the mode quality of the laser. Further, by using the AOM as the active Q switch, the repetition rate of the laser pulse and the pulse width could be accurately adjusted within a wide range even at any fixed value of the pump power above the lasing threshold, undoubtedly this feature of the pulse parameters would significantly extend the operational advantage of the laser for some practical applications especially like metal cutting and welding. In our experiment, the laser could be continuously adjusted from 500 Hz to 9.238 kHz at different pump powers, with pulse duration in the range of 26.4–67.2 ns and the peak power in the range of 2–7.75 kW. The detailed work is described in the following sections.

## 2 Experimental setup

Figure 1 schematically shows the experimental setup. The pumping light from a fiber-coupled 808-nm LD was focused into the crystal. The laser resonator consisted of a plane mirror, a diffusion-bonded Nd:YAG crystal, an AOM, and a sub-wavelength grating mirror. The distance between M1 to the front surface of bonded crystal was 13.5 mm, and the total length of the laser cavity was 100 mm. The plane mirror M1 was coated for high transmission at 808 nm and high reflection at 1064 nm. The used Nd:YAG crystal was 2-mm thick and 1-at.% doped, and it was bonded with two 3-mm thick and undoped YAG end caps. The front surface of the bonded crystal was coated for high transmission at both 808 nm and 1064 nm, while the rear surface was antireflection-coated at 1064 nm. The crystal was sandwiched in between two flat copper plates, and there was a 2-mm-diameter tunnel drilled along the cavity axis in each copper. The front copper plate was connected to a 23°C water cooling. The AOM, which exhibited polarization-independent transmission, was a 5.22-cm-thick, antireflection-coated fused silica cube with nearly plane parallel surfaces, driven at frequencies of 0.5–9 KHz.

The subwavelength grating mirror used as the output coupler had a multilayer structure that composed of high-

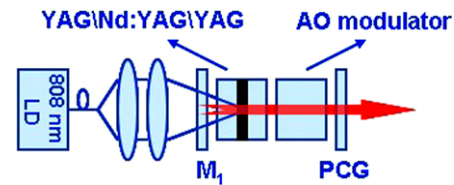


**Fig. 1** Experimental setup of the LD end-pumped and bonded Nd:YAG laser

and low-refractive-index layers with each layer alternately shaped into concentric corrugations (groove). The concentric and multilayer structure induced the artificial birefringence and resonant interference, and by proper design to the grating parameters like the layer thickness and numbers, groove pitch, and others, the grating could show desired transmittance or reflectance to both the transverse electric (TE, polarization parallel to grating groove) and transverse magnetic (TM, polarization orthogonal to grating groove) waves. In our experiment, the photonic crystal grating used as output coupler had a reflectivity of about 90% for TM wave and was transparent to TE wave at 1064 nm [27–31].

## 3 Experimental results and discussions

In the experiment, it was observed that for a given pump power, with the increase of the driven frequency of the AO modulator, the measured laser repetition rate grew to a maximum value, then, it became unstable and dropped quickly, and finally, no pulse signals were detected. To verify this phenomenon, the experiment was carried on under several different pumping powers. For comparison and convenience, the output properties of the laser pulses were only discussed on the following three pumping powers, namely as 10.8 W, 11.5 W, and 12.6 W.

Figure 2 shows the measured laser powers of the actively Q-switched Nd:YAG laser as functions of measured repetition rate under three different pumping powers. The maximum output powers were 0.193 W, 0.395 W, and 0.72 W at the pumping powers of 10.8 W, 11.5 W, and 12.6 W, respectively. The corresponding optical-to-optical (o–o) efficiencies were about 1.79%, 3.43%, and 5.71%. (Because the central wavelength of the LD used here deviated from the absorption peak of the lasing material, the o–o efficiency was not extremely high.) The repetition rates begun with 500 Hz and are identical to the minimum smallest driven frequency of the AO modulator. The error between the measured repetition rates and the driven frequency was less than 10 Hz. The laser repetition rates became unstable when the driven frequency exceeded 9.00 kHz, 5.47 kHz, and 2.51 kHz at the different pump powers of 12.6 W, 11.5 W, and 10.8 W, respectively. As can be seen, at low repetition rates the average laser power is approximately proportional

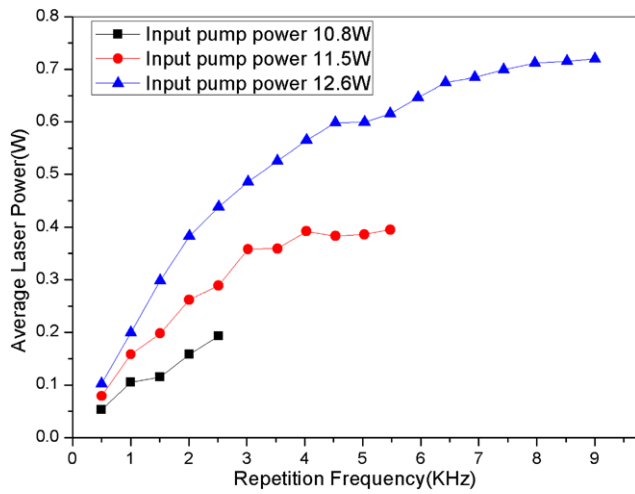


**Fig. 2** Laser powers as functions of the measured repetition rates at different pump powers

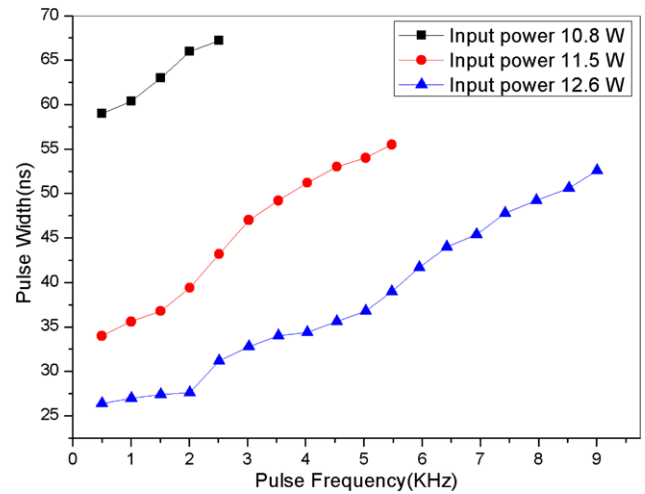


**Fig. 3** Pulse widths as functions of the measured repetition rates at different pump powers

to the repetition rate, but above a certain repetition rate, the Q-switch average power gradually approached a maximum value. When continuously increasing the driven frequency of the AO modulator, the measured repetition rates became unstable and dropped quickly to zero.

Figure 3 depicts the measured width of laser pulse as a function of measured repetition rate at different pump powers. As seen, the pulse durations increased from 26.4 ns, 34 ns, and 59 ns with the repetition rate and reached 52.6 ns, 55.5 ns, and 67.2 ns at the pump powers of 12.6 W, 11.5 W, and 10.8 W, respectively. Figure 4 shows the captured pulse envelope and trains at pump powers of 12.6 W, where the pulse width (FWHM) is 52.6 ns with a repetition rate of 9.238 kHz. It was observed that there existed a large pulse-to-pulse amplitude fluctuation in the measured pulse trains, and such fluctuation may result from the disturbing of ther-

mal lensing effect to the metastable condition of the used flat-to-flat cavity resonator. Therefore, the further improvement to the pulse stability can be expected by using flat-concave or double-concave cavity design.

Furthermore, we calculated the laser pulse's peak power and energy pulse by using the measured pulse parameters (the averaged power, repetition rates, and pulse widths and thereafter plotted them as functions of the measured repetition rate in Fig. 5. As seen, the peak powers gradually decreased from 7.75 kW, 4.66 kW, and 1.80 kW to 1.52 kW, 1.30 kW, and 1.41 kW with the increase of the repetition rate, and meantime the pulse energies decreased from 205  $\mu$ J, 159  $\mu$ J, and 498  $\mu$ J to 80  $\mu$ J, 72  $\mu$ J, and 77  $\mu$ J, at the pump powers of 12.6 W, 11.5 W, and 10.8 W, respectively.

The laser beam was observed to show doughnut-shape profile. Figures 6(a) and (b) gave the far- and near-field full

**Fig. 4** Observed oscilloscope traces of (top) pulse envelope and (bottom) laser pulse train

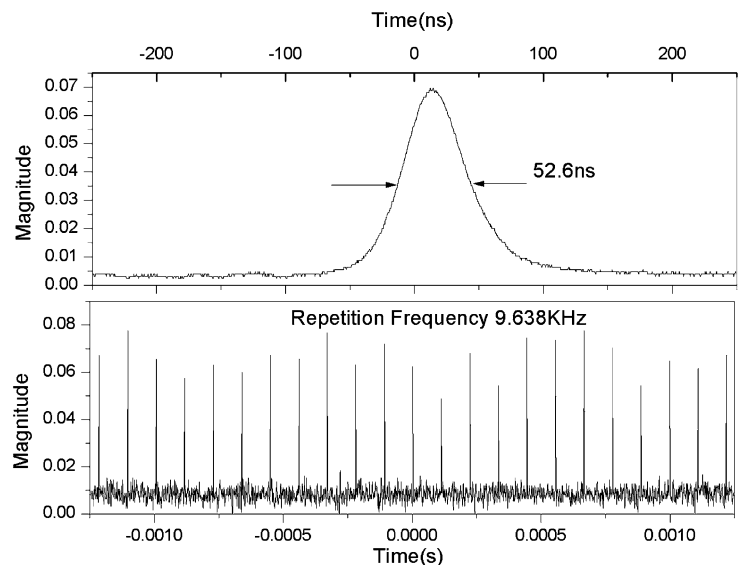
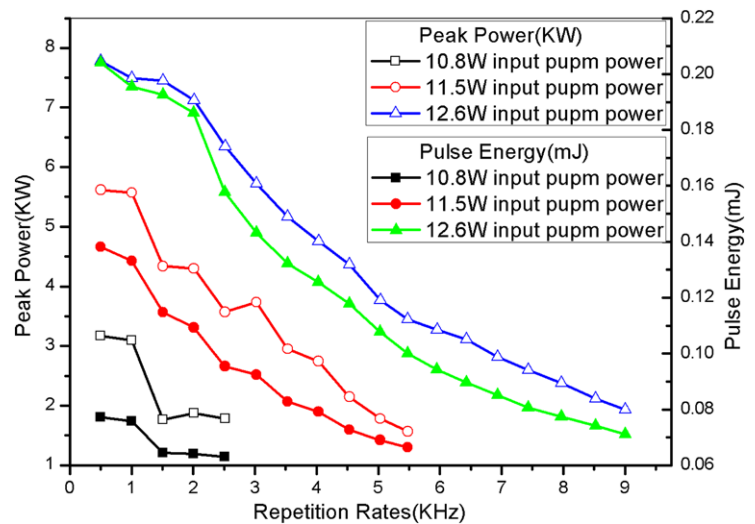


**Fig. 5** Pulse peak powers and pulse energies as functions of the measured repetition rates at different pump powers



profiles of laser beams at 9-kHz repetition rate and 12.6-W pump power, where a doughnut-shaped cross section with a central null was clearly discerned. The polarization state of laser beam was also analyzed by placing a polarizer in front of the CCD camera. Figures 6(c)–(f) depicted the corresponding far-field intensity distribution of the passage beam from the analyzer at different orientations of the analyzer's axes. As a result, when rotating the analyzer, it was observed that the transmitted beam profile, the two-lobe structure, in each image was always identical to the corresponding axis direction of the analyzer, and this certifies that the obtained laser beam was radially polarized.

It also was observed that there existed a vertical dark line in the full beam profile of Fig. 6. It was already reported by several groups that the laser output from the Q switched Nd:YAG crystal laser or CW Yb:YAG crystal laser was linearly polarized without any polarization-dependent element inside the laser cavity [32, 33]. In general, it is believed that the crystalline-orientation of YAG crystal during the crystal growth is responsible for this self polarization and causes the YAG crystal to become anisotropic in the laser application. Therefore, the vertical dark line in the full beam profile given in Fig. 6 could be contributed to such anisotropic effect of YAG crystal.

The polarization purity of the obtained laser beam was also measured based on the following principle. At every point along the ring profile of an ideal radially polarized light, the local polarization state is linearly polarized along the respective radial direction, and thus polarization extinction ratio (PER) of this point could represent that of the whole ring laser beam. Based on this principle, a 200- $\mu$ m-diameter aperture was placed into the optical path at a distance of 1.5 m behind the grating mirror, and the aperture's position was adjusted laterally to maximize the intensity of the transmitted light; then the PER of the transmitted light

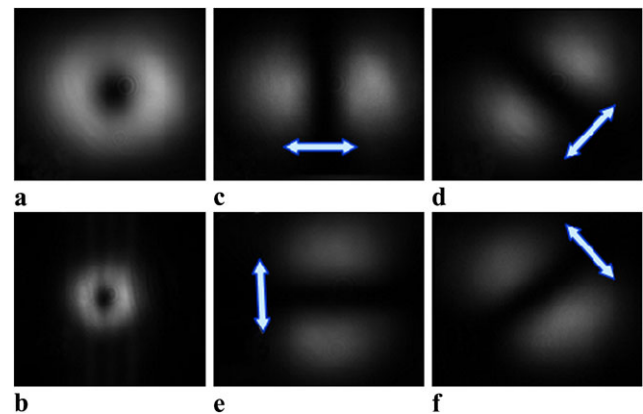


**Fig. 6** (a) Far- and (b) near-field intensity distributions of the full beam profile; (c)–(f) variations of far-field intensity distributions of the passage beam through the polarizer analyzer at different orientations of the polarizer axes (where white arrows indicate the directions of the polarizer analyzer's axis)

through the aperture could be measured by rotating the polarization analyzer. By this way, we acquired a PER of 78:1, and this corresponds to a polarization purity (degree) of 97.4%.

It is worthwhile to point out that though the laser cavity used by us was a flat–flat mirror configuration, which had a metastable nature, and therefore the thermal-lens effect could be a problem at high pumping power. In our case, though the cavity length was 100 mm and seems to be a little long, we used a composite structure of gain medium (YAG + Nd:YAG + YAG) which could alleviate the thermal lensing effect significantly in the presence of the active water cooling. As a result, we still obtained the stable pulse lasing when the pump power was less than 12.6 W at a driven frequency of AOM less than 9.238 kHz. When the pump power was a little larger than 12.6 W, the annular profile of the laser mode became diffused.

To check the validity of bonded gain medium for alleviating the thermal lens effect, we also used a 2-mm-thick Nd:YAG crystal (nonbonded), directly replaced the composite YAG + Nd:YAG + YAG crystal, and simultaneously kept the other conditions (cooling, coating, and cavity length) unchanged, and we did not obtain the lasing at any pump power.

#### 4 Conclusion

In summary, we achieved repetition-rate-controllable pulsed radially polarized beams from an actively Q-switched Nd:YAG laser with a photonic crystal grating as the output coupler. By use of an acousto-optic Q switch and a bonded structure crystal, the laser emitted high peak-power and small repetition rates fluctuation pulses with high laser polarization purity.

**Acknowledgements** This research is sponsored by National Science Foundation of China (60978025), Hundred Talents Program of CAS and Shanghai Pujiang Program (09PJ1410500). Kegui Xia thanks Di Lin, Zhiqiang Fang, Minqiang Kang, and Lei Xiao for discussion and help for the experiment. Jianlang Li acknowledges Dr. Takashi Sato and Antony Galea from Photonic Lattice Inc. for their supports in the grating mirrors.

#### References

1. T.A. Nieminen, N.R. Heckenberg, H. Rubinsztein-Dunlop, *Opt. Lett.* **33**, 122 (2008)
2. T. Kuga, Y. Torii, N. Shiokawa, T. Hirano, Y. Shimizu, H. Sasada, *Phys. Rev. Lett.* **78**, 4713 (1997)
3. Q. Zhan, *Opt. Express* **12**, 3377 (2004)
4. W.D. Kimura, G.H. Kim, R.D. Romea, L.C. Steinhauer, I.V. Pogorelsky, K.P. Kusche, R.C. Fernow, X. Wang, Y. Liu, *Phys. Rev. Lett.* **74**, 546 (1995)
5. R. Dorn, S. Quabis, G. Leuchs, *Phys. Rev. Lett.* **91**, 233901 (2003)
6. V.G. Niziev, A.V. Nesterov, *J. Phys. D, Appl. Phys.* **32**, 1455 (1999)
7. M. von Bostel, in *Stuttgart Laser Technology Forum (SLT'10)*, Stuttgart, Germany (2010)
8. T. Moser, M.A. Ahmed, M. Schäfer, M.M. Vogel, A. Voss, Th. Graf, in *Stuttgart Laser Technology Forum (STL'08)*, Stuttgart, Germany (2008)
9. M. Meier, V. Romano, T. Feurer, *Appl. Phys. A, Mater. Sci. Process.* **86**, 329 (2007)
10. M. Kraus, M.A. Ahmed, A. Michalowski, A. Voss, R. Weber, T. Graf, *Opt. Express* **18**, 2305 (2010)
11. Y. Mushiaki, K. Matsumura, N. Nakajima, *Proc. IEEE* **60**, 1107 (1972)
12. T. Moser, M.A. Ahmed, F. Pigeon, O. Parriaux, E. Wyss, T. Graf, *Laser Phys. Lett.* **1**, 234 (2004)
13. G.M. Lerman, U. Levy, *Opt. Lett.* **33**, 2782 (2008)
14. Y. Kozawa, S. Sato, T. Sato, Y. Inoue, Y. Ohtera, S. Kawakami, *Appl. Phys. Express* **1**, 022008 (2008)
15. J.L. Li, K.I. Ueda, M. Musha, L.X. Zhong, A. Shirakawa, *Opt. Lett.* **33**, 2686 (2008)
16. D. Lin, K.G. Xia, J.L. Li, R.X. Li, K.I. Ueda, G.Q. Li, X.J. Li, *Opt. Lett.* **35**, 2290 (2010)
17. J.-F. Bisson, J.L. Li, K.I. Ueda, Y. Senatsky, *Opt. Express* **14**, 3304 (2006)
18. Y. Kozawa, S. Sato, *Opt. Lett.* **30**, 3063 (2005)
19. K. Yonezawa, Y. Kozawa, S. Sato, *Opt. Lett.* **31**, 2151 (2006)
20. S.C. Tidwell, G.H. Kim, W.D. Kimura, *Appl. Opt.* **32**, 5222 (1993)
21. G. Volpe, D. Petrov, *Opt. Commun.* **237**, 89 (2004)
22. M.A. Ahmed, J. Schulz, A. Voss, O. Parriaux, J.-C. Pommier, T. Graf, *Opt. Lett.* **32**, 1824 (2007)
23. M.A. Ahmed, M. Haefner, M. Vogel, C. Pruss, A. Voss, *Opt. Express* **19**, 509 (2011)
24. D. Lin, K.G. Xia, R.X. Li, X.J. Li, G.Q. Li, K.I. Ueda, J.L. Li, *Opt. Lett.* **35**, 3574 (2010)
25. F. Enderli, T. Feurer, *Opt. Lett.* **34**, 2030 (2009)
26. M. Meier, V. Romano, T. Feurer, *Appl. Phys. A* **86**, 329 (2007)
27. Y. Kozawa, S. Sato, T. Sato, Y. Inoue, Y. Ohtera, S. Kawakami, *Appl. Phys. Express* **1**, 022008 (2008)
28. S. Kawakami, T. Kawashima, T. Sato, *Appl. Phys. Lett.* **74**, 463 (1999)
29. A. Mehta, J.D. Brown, P. Srinivasan, R.C. Rumpf, E.G. Johnson, *Opt. Lett.* **32**, 1935 (2007)
30. S. Kawakami, *Electron. Lett.* **33**, 1260 (1997)
31. J.L. Li, K.I. Ueda, L.X. Zhong, M. Musha, A. Shirakawa, T. Sato, *Opt. Express* **16**, 10841 (2008)
32. J. Dong, A. Shirakawa, K. Ueda, *Appl. Phys. Lett.* **93**, 101105 (2008)
33. S. Zhou, K.K. Lee, Y.C. Chen, S. Li, *Opt. Lett.* **18**, 511 (1993)